

1999

## Analysis of Sub-Interface Cracks

C.T. Liu  
AFRL/PRSM  
10 E. Saturn Blvd  
Edwards AFB CA 93524-7680

L. Wang & S.N. Atluri  
Center for Aerospace Research and Education  
University of California, Los Angeles  
Los Angeles, CA 90095-1600

### Abstract

In this study, linear elastic finite element analyses were conducted to analyze a bonded specimen with a sub-interface crack. The effects of the adhesive layer's thickness and stiffness, the initial sub-interface crack length, and the location of the sub-interface crack, on the stress intensity factors at the tip of the sub-interface crack were investigated. The results of the analyses are discussed.

### Introduction

Bonded sandwich laminates are being used widely in various industries. Both primary and secondary structural components in aircraft and space vehicles are made of such composites. They also have been successfully used in pipes, chemical tanks, ship hulls, and in other structural applications in which a high strength-to-weight ratio is a desirable feature.

An important engineering problem in structural design is the evaluation of structural integrity and reliability. It is well known that structural strength may be degraded during its design life due to mechanical or chemical aging, or a combination of these two aging mechanisms. Depending on the structural design, material type, service loading, and environmental condition, the cause and degree of strength degradation due to the different aging mechanisms differ. One of the common causes of strength degradation in bonded structures is the development of cracks in or near the interfaces of the structures.

During the past years, a considerable amount of work has been done in studying interfacial fracture in bimetals. Comprehensive overviews on two-dimensional elastic fracture mechanics of interfaces were given by Rice ( 1 ) and Hutchinson and Suo ( 2 ). The elastic-plastic fields near bimaterial crack tip under small scale yielding conditions were investigated by Shih and Asaro ( 3 ), and Zywickz and Parks ( 4 ). The stress fields near the tip of a crack in the interfaces between viscoelastic solids were determined by Knauss ( 5 ). An experimental study of an interface crack in bimetals was conducted by Yan and Chiang ( 6 ). The effects of material mismatch on the interfacial stress intensity

20000830 089

factor of bonded systems were studied by Smith ( 7 ) and Miller ( 8 ). The stress intensity factors at the tip of a crack paralleling an interface between dissimilar materials with zero thickness of the adhesive layer were determined by Hutchinson et.al.( 9 ), and Smith et. al. ( 10 ). And Beom and Atluri(11)

In this study, the stress intensity factors at the tip of a sub-interface crack, which is parallel to and near the interface of a bonded system, were determined, using the Schwartz-Neumann type finite element alternating method. The effects of the initial sub-interface crack length, the thickness and modulus of the adhesive layer, and the distance between the crack and the interface on the stress intensity factors were investigated and the results are discussed.

### **Numerical Modeling**

In this study, computational models, based on the Schwartz-Neumann type finite element alternating method (FEAM), was used to perform fracture analyses of a bonded specimen. The geometry of the specimen is shown in Fig.1 The Young's Modulus of material-1 is 700 psi and the Poisson Ratio is 0.4999. Three different moduli ( 100 psi, 700 psi, and 1000 psi ) of the adhesive material were considered, and the poisson ratio of the adhesive material is 0.4999. A total of 18 cases were analyzed as shown in Table 1. In cases 1 and 2, the adhesive layers have the same material properties as material 1. In cases 3-10, the adhesive layers have a smaller Young's Modulus than that of Material 1. In cases 11-18, the adhesive layers have a larger Young's Modulus than that of material 1. Since in cases 1 and 2, the adhesive layers have the same material properties as material 1, the specimens are homogeneous specimens. For all the cases analyzed, the specimen was subjected to a constant displacement of 0.037 in and linearly elastic analyses was performed.

Since the FEAM uses an analytical solution for a single crack in an infinite homogeneous sheet, the FEAM is limited to analyze the fracture of a homogeneous isotropic material. In order to overcome this limitation, a global-local analysis approach was used. In the global model, a simple finite element model (FEM) was used to model the entire specimen, where the crack was modeled using disconnected nodes in a coarse mesh. A global analysis was used to capture the load flow in the specimen. A local model, which contained only a single material and the sub-interface crack, was extracted from the global analysis. The local model was analyzed using the finite element alternating method, which does not require the explicit modeling of the crack using a FEM mesh. Fracture parameters were obtained from the local analyses.

In the analyses, both AL end tabs and the specimen were included in the global model. Cracks were modeled using disconnected nodes in the global model. The tractions and the displacements along the interface, between the adhesive layer and Material 1 that contains the sub-interface crack, were determined from the global analysis. These tractions and displacements were used as the boundary conditions for the local model.

In the analysis, the stress intensity factors (SIF) were calculated, based on the FEAM. In Addition, the traction along the interface between the AL end tab and Material 1 was integrated to obtain the total applied force on the specimen. The computed Mode I SIF  $K_I$  is normalized with respect to Mode I  $K_{I0}$ , which is defined as

$$K_{I0} = (P/wt)(\pi a)^{1/2}$$

where  $P$  is the total applied force in  $y$  direction;  $w$  is the width of test panel; and  $t$  is the thickness of the specimen which is equal to 0.5 in;  $a$  is the length of the crack.

### Computational Results

The results of the analyses are shown in Table 2 and figures 2-4. For the two special cases (cases 1 and 2), the normalized Mode I SIF ( $K_I/K_{I0}$ ) for the specimen subjected to a uniform displacement is shown as the solid line in Fig.2. It is obtained by using Finite Element Alternating Method directly. The diamond points show the normalized Mode I SIF ( $K_I/K_{I0}$ ) obtained using the global approach, including the Al end tabs in the finite element model. A very good agreement is shown in Fig.2. This validates the accuracy of the global-local approach.

The broken line in Fig.2 shows the normalized Mode I SIF ( $K_I/K_{I0}$ ) for the specimen subjected to a uniform far field stress. It is seen that under the uniform displacement boundary condition, the normalized Mode I SIF ( $K_I/K_{I0}$ ) decreases with increasing the crack length. However, under the uniform stress boundary condition, the normalized Mode I SIF increases as the crack length is increased.

When the adhesive layer is softer than the adhered material (cases 3-10), the normalized Mode I SIFs are larger than those of the specimens made of homogenous material as shown in Fig.3. This indicates that a softer adhesive layer can result in a higher normalized Mode I SIF. It is also seen that the thicker the adhesive layer, the larger the effect of the adhesive layer on the normalized Mode I SIF. In addition, when the crack is away from the interface (i.e. for larger  $d$ ), the effect of the adhesive layer on the normalized Mode I SIF is smaller.

When the adhesive layer is stiffer than the adhered material, the normalized Mode I SIFs are almost the same as those of the specimens made of homogenous material as shown in Fig.4. This indicates that the effect of the adhesive layer on the Mode I SIF is negligible

### Conclusion

In this study, numerical analyses, based on finite element alternating methods, were conducted to investigate the effects of adhesive layer's stiffness and thickness on the stress intensity factors at the tip of a sub-interface crack which is near the interface

between the adhesive layer and the adhered material. For all the cases analyzed, the Mode II stress intensity factor is negligibly small. However, for Mode I stress intensity factor, the normalized stress intensity factor is affected by the stiffness and the thickness of the adhesive layer. The results reveal that, by comparing with the homogeneous specimen, a softer adhesive layer results in a higher normalized Mode I stress intensity factor, whereas there is no significant effect on the normalized Mode I stress intensity factor if the adhesive layer is stiffer. It also reveals that, for a soft adhesive layer, the normalized Mode I SIF increases with increasing the thickness of the adhesive layer. However, for a stiffer adhesive layer, the effect of the thickness of the adhesive layer on the normalized Mode I SIF is relatively small.

### References

- (1) Rice, J.R.( 1988 ), "Elastic Fracture mechanics Concepts for Interfacial Cracks," ASME Journal of Applied Mechanics, Vol. 55, pp98-103.
- (2) Hutchinson, J. W. and Suo, Z., "Mixed Mode Cracking in Layered Materials," Advanced in Applied mechanics, Vol.28.
- (3) Shih, C.F. and Asaro, R.J.( 1988 ), " Elastic-Plastic Analysis of Cracks on Bimaterial Interfaces: PartI- Small Scale Yielding," ASME Journal of Applied Mechanics, Vol. 55, pp.299-316.
- (4) Zywickz, E. and Parks, D.M. ( 1990 ), " Elastic-Plastic Analysis of Frictionless Contact at Interfacial Crack Tips," International Journal of Fracture, Vol. 42, PP. 129-143.
- (5) Geubelle, P.H. and Knauss, W.G. (1995), " Crack Propagation in Homogeneous and Bimaterial Sheet under General In-Plane Loading," ASME Journal of Applied Mechanics, Vol. 62, pp. 601-606.
- (6) Chiang, F.P., Yan, X. T. and Lu, H. ( 1992 ), " Measurement of Three-dimensional Deformation of an Interfacial Crack in a Bimaterial," Engineering Fracture Mechanics, Vol.43, No.1, pp.101-106.
- (7) Smith, C.W., Finlayson, E.F. and Liu, C.T. (1997), " A method for Evaluating Stress Intensity Distribution for Cracks in Rocket Motor Bondlines," Engineering Fracture Mechanics, Vol.58, No.2, pp.97-105.
- (8) Miller, T.C. (1999), " Modeling of Plane Strain Interfacial Fracture In Incompressible Materials," Composites Part B: Engineering, Vol.30, pp.291-296.
- (9) Hutchinson, J.W., Mear, M.E. and Rice, J.R. (1987 ), " Crack Paralleling an Interface between Dissimilar Materials," ASME Journal of Applied Mechanics, Vol. 54, pp.828-832.
- (10) Smith, C.W. and Liu, C.T. (1999 ), " Material Influences on the Estimation of Bond Line Effects on Stress Intensity Factors for Cracks Parallel to and within Bondlines by the Frozen Stress method," Proceeding of the Eighth International Conference on the Mechanical behavior of Materials, Victoria, B.C. Canada, Vol.1 pp.244-248.
- (11) Beom, H. G, and Atluri, S.N (1995) "Asymptotic Analysis of a Subinterface Crack in Dissimilar Orthotropic Media", Eng. Fracture Mech. 52: (5) 777-790

Table. 1 Definitions of the Analysis Cases

| No. | E (psi) | h (in) | d (in) | a (in) | No. | E (psi) | h (in) | d (in) | a (in) |
|-----|---------|--------|--------|--------|-----|---------|--------|--------|--------|
| 1   | 700     | 0.10   | 0.15   | 0.10   | 11  | 1000    | 0.05   | 0.15   | 0.10   |
| 2   | 700     | 0.10   | 0.15   | 0.50   | 12  | 1000    | 0.05   | 0.15   | 0.50   |
| 3   | 100     | 0.05   | 0.15   | 0.10   | 13  | 1000    | 0.05   | 0.30   | 0.10   |
| 4   | 100     | 0.05   | 0.15   | 0.50   | 14  | 1000    | 0.05   | 0.30   | 0.50   |
| 5   | 100     | 0.05   | 0.30   | 0.10   | 15  | 1000    | 0.20   | 0.15   | 0.10   |
| 6   | 100     | 0.05   | 0.30   | 0.50   | 16  | 1000    | 0.20   | 0.15   | 0.50   |
| 7   | 100     | 0.20   | 0.15   | 0.10   | 17  | 1000    | 0.20   | 0.30   | 0.10   |
| 8   | 100     | 0.20   | 0.15   | 0.50   | 18  | 1000    | 0.20   | 0.30   | 0.50   |
| 9   | 100     | 0.20   | 0.30   | 0.10   |     |         |        |        |        |
| 10  | 100     | 0.20   | 0.30   | 0.50   |     |         |        |        |        |

Table. 2 Summary of the Analysis Results

| No. | E (psi) | h (in) | d (in) | a (in) | $K_I/K_{I_0}$ | No. | E (psi) | h (in) | d (in) | a (in) | $K_I/K_{I_0}$ |
|-----|---------|--------|--------|--------|---------------|-----|---------|--------|--------|--------|---------------|
| 1   | 700     | 0.10   | 0.15   | 0.10   | 0.8958        | 11  | 1000    | 0.05   | 0.15   | 0.10   | 0.8918        |
| 2   | 700     | 0.10   | 0.15   | 0.50   | 0.8702        | 12  | 1000    | 0.05   | 0.15   | 0.50   | 0.8636        |
| 3   | 100     | 0.05   | 0.15   | 0.10   | 0.9795        | 13  | 1000    | 0.05   | 0.30   | 0.10   | 0.9083        |
| 4   | 100     | 0.05   | 0.15   | 0.50   | 0.9187        | 14  | 1000    | 0.05   | 0.30   | 0.50   | 0.8648        |
| 5   | 100     | 0.05   | 0.30   | 0.10   | 0.9551        | 15  | 1000    | 0.20   | 0.15   | 0.10   | 0.8972        |
| 6   | 100     | 0.05   | 0.30   | 0.50   | 0.9134        | 16  | 1000    | 0.20   | 0.15   | 0.50   | 0.8699        |
| 7   | 100     | 0.20   | 0.15   | 0.10   | 1.1429        | 17  | 1000    | 0.20   | 0.30   | 0.10   | 0.9137        |
| 8   | 100     | 0.20   | 0.15   | 0.50   | 1.0478        | 18  | 1000    | 0.20   | 0.30   | 0.50   | 0.8720        |
| 9   | 100     | 0.20   | 0.30   | 0.10   | 1.0687        |     |         |        |        |        |               |
| 10  | 100     | 0.20   | 0.30   | 0.50   | 1.0401        |     |         |        |        |        |               |

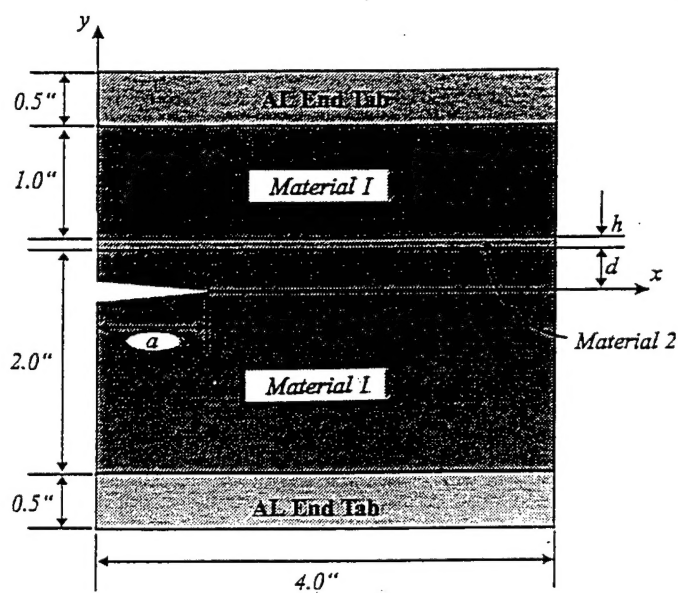


Fig. 1 Specimen geometry.

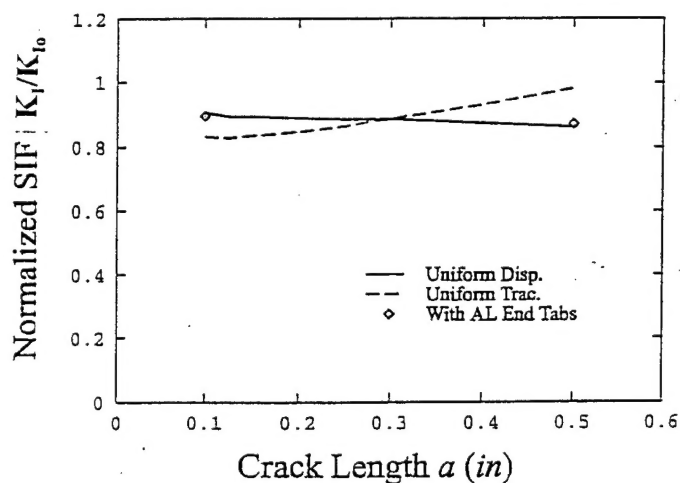


Fig. 2 Normalized SIF versus crack length (adhesive layer has same material property as material 1).

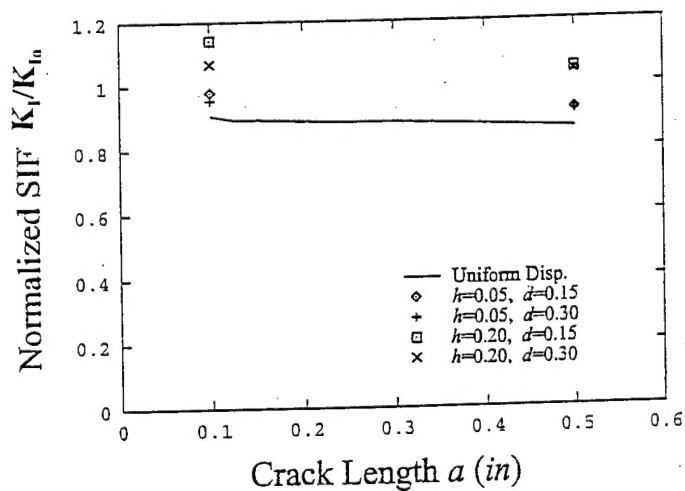


Fig. 3 Normalized SIF versus crack length (adhesive layer is softer than material 1).

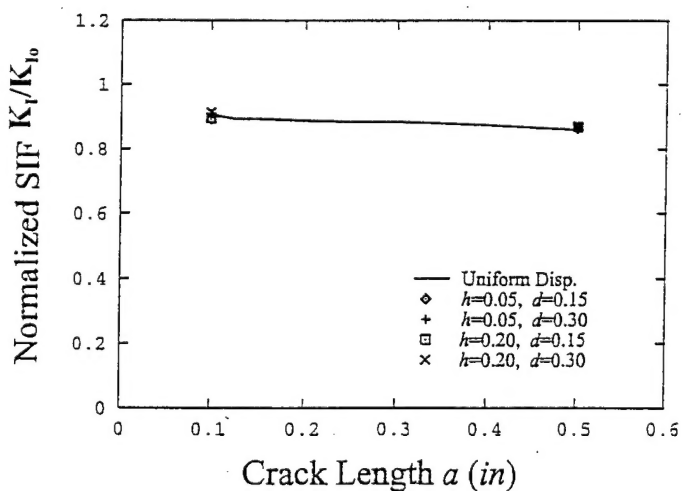


Fig. 4 Normalized SIF versus crack length (adhesive layer is stiffer than material 1).